HHS Public Access

Author manuscript

Arterioscler Thromb Vasc Biol. Author manuscript; available in PMC 2016 November 01.

Published in final edited form as:

Arterioscler Thromb Vasc Biol. 2015 November ; 35(11): 2391–2400. doi:10.1161/ATVBAHA.115.306474.

Fibronectin splicing variants containing extra domain A promote atherosclerosis in mice through Toll-like receptor 4

Prakash Doddapattar[1,$], **Chintan Gandhi**[1,$,#], **Prem Prakash**[1], **Nirav Dhanesha**[1], **Isabella M. Grumbach**[1], **Michael E. Dailey**[2], **Steven R. Lentz**[1], and **Anil K. Chauhan**[1]

[1]Department of Internal Medicine, University of Iowa, Iowa City, IA

[2]Department of Biology, University of Iowa, Iowa City, IA

Abstract

Objective—Cellular fibronectin containing extra domain A (EDA$^+$-FN) is abundant in the arteries of patients with atherosclerosis. Several *in vitro* studies suggest that EDA$^+$-FN interacts with Toll-like receptor 4 (TLR4). We tested the hypothesis that EDA$^+$-FN exacerbates atherosclerosis through TLR4 in a clinically-relevant model of atherosclerosis, the apolipoprotein E-deficient (*Apoe*$^{-/-}$) mouse.

Approach and Results—The extent of atherosclerosis was evaluated in whole aortae and cross sections of the aortic sinus in male and female *EDA*$^{-/-}$*Apoe*$^{-/-}$ mice (which lack EDA$^+$-FN), *EDA*$^{fl/fl}$*Apoe*$^{-/-}$ mice (which constitutively express EDA$^+$-FN) and control *Apoe*$^{-/-}$ mice fed a high-fat "Western" diet for 14 weeks. Irrespective of gender, *EDA*$^{fl/fl}$*Apoe*$^{-/-}$ mice exhibited a 2-fold increase in atherosclerotic lesions (aorta and aortic sinus) and macrophage content within plaques, whereas *EDA*$^{-/-}$*Apoe*$^{-/-}$ mice exhibited reduced atherosclerotic lesions ($P<0.05$ vs. *Apoe*$^{-/-}$, n=10-12 mice/group), although cholesterol and triglyceride levels, and circulating leukocytes were similar. Genetic ablation of TLR4 partially reversed atherosclerosis exacerbation in *EDA*$^{fl/fl}$*Apoe*$^{-/-}$ mice ($P<0.05$) but had no effect on atherosclerotic lesions in *EDA*$^{-/-}$*Apoe*$^{-/-}$ mice. Purified cellular FN, which contains EDA, potentiated dose-dependent NFκB-mediated inflammation (increased phospho-NFκB p65/ NFκB p65, TNFα and IL1β) in bone marrow-derived macrophages from *EDA*$^{-/-}$*Apoe*$^{-/-}$ mice but not from *EDA*$^{-/-}$*TLR4*$^{-/-}$*Apoe*$^{-/-}$ mice. Finally, using immunohistochemistry, we provide evidence for the first time that EDA$^+$-FN colocalizes with macrophage TLR4 in murine aortic lesions and human coronary artery atherosclerotic plaques.

Conclusions—Our findings reveal that TLR4 signaling contributes to EDA$^+$-FN mediated exacerbation of atherosclerosis. We suggest that EDA$^+$-FN could be a therapeutic target in atherosclerosis.

Corresponding author: Anil K. Chauhan, Ph.D., University of Iowa, Department of Internal Medicine, 25 S. Grand Avenue, 3188 Medical labs, Iowa City, Iowa-52242, Telephone: 319-335-6525, Fax: 319-353-8383, anil-chauhan@uiowa.edu.
[#]Current address: Center for Vascular and Inflammatory Diseases, School of Medicine, University of Maryland, Baltimore-MD
[$]These authors contributed equally to the article.

Disclosures

None.

Keywords

Cellular fibronectin EDA; atherosclerosis; TLR4

Introduction

Atherosclerosis is a chronic inflammatory disease that affects large arteries and is characterized by plaques composed of lipids, calcium, extracellular matrix (ECM) and inflammatory cells including monocytes/macrophages, T lymphocytes and neutrophils. Much of the morbidity and mortality associated with atherosclerosis is due to coronary artery plaques, which cause luminal obstruction due to vessel stenosis and occlusive thrombus triggered by rupture of unstable plaques. During progression of atherosclerosis, extensive remodeling of ECM takes place. Several studies have found that altered ECM participates at different stages of atherosclerosis.[1, 2] There is emerging evidence that in chronically inflamed tissues, aberrant expression of ECM proteins or ECM fragments can modulate migration of leukocytes and immune cell responses at these sites.[3] In healthy human arteries, the endothelium resides on an ECM that is mainly composed of collagen type IV and laminin. In contrast, the ECM of atherosclerotic arteries contains abundant deposits of fibronectin (FN) in both humans and murine models,[4-7] suggesting a functional role for FN in the pathophysiology of atherosclerosis.

FN is a dimeric glycoprotein that is known to play an important role in several cellular processes.[8] FN exhibits diversity at the protein level as a consequence of alternative splicing of a single primary transcript at three exons that encode the Extra Domain A, the Extra Domain B and the Type III Homologies Connecting Segment. The major isoform of FN found in plasma lacks both the alternatively-spliced extra domain A and extra domain B segments, and is synthesized by hepatocytes. The predominant isoform of FN found in the ECM, which is known as “cellular FN,” contains the extra domain A and/or extra domain B segments. Cellular FN in the ECM is synthesized by vascular cells, including endothelial and vascular muscle cells.[8] The amino acid sequence of the EDA is highly conserved (> 90%) in mammals, as is its splicing pattern, with either total inclusion or exclusion of the EDA observed in mice, rats, and humans.[9] Inclusion of the EDA exon in FN gene by alternative splicing is specifically regulated during several biological and pathological processes, including cutaneous wound healing,[10, 11] vascular intimal proliferation,[12] vascular hypertension,[13] cardiac transplantation, [14] and fibrosis of the lung, liver and kidney, [15-17] suggesting a functional role for EDA^+-FN in these biological processes.

FN variants containing EDA (EDA^+-FN) are specifically expressed in atherosclerotic but not healthy arteries, suggesting a possible functional role for EDA^+-FN in atherosclerosis.[12, 18] Two prior studies have found that deletion of the EDA exon of the FN gene reduces atherosclerotic plaque progression in mice,[18, 19] but the mechanisms underlying these observations remain obscure. *In vitro* studies have suggested that EDA, but not other domains of FN, activates Toll-like-receptor 4 (TLR4) signaling.[20] In agreement with this finding, our group reported recently that a pharmacological inhibitor of TLR4 (TAK-242) prevented the ability of EDA^+-FN to exacerbate ischemia/reperfusion injury in

the brain.[21] Recently, it was shown that EDA$^+$-FN interacts with TLR4 and promotes chronic cutaneous fibrosis through TLR4 signaling.[22] Given that TLR4 is known to modulate progression of atherosclerosis,[23] these findings provided a compelling rationale to test the hypothesis that EDA$^+$-FN promotes atherosclerosis through the TLR4 signaling pathway. We generated following strains of atherosclerotic *Apoe*$^{-/-}$ mice: 1) *EDA*$^{fl/fl}$*Apoe*$^{-/-}$ mice, which constitutively express EDA$^+$-FN; 2) *EDA*$^{-/-}$*Apoe*$^{-/-}$ mice, which completely lack EDA$^+$-FN; 3) *EDA*$^{fl/fl}$*TLR4*$^{-/-}$*Apoe*$^{-/-}$ mice, which constitutively express EDA$^+$-FN but lack TLR4; 4) *EDA*$^{-/-}$*TLR4*$^{-/-}$*Apoe*$^{-/-}$ mice, which lack EDA$^+$-FN and TLR4; and 5) *TLR4*$^{-/-}$*Apoe*$^{-/-}$ mice, which lack TLR4; and 6) control *Apoe*$^{-/-}$ mice, which express low levels of EDA^{+-}FN as well as other FN splicing variants.

Herein, we provide evidence for the first time that TLR4 contributes to EDA$^+$-FN mediated atherosclerosis exacerbation in *Apoe*$^{-/-}$ mice. Furthermore, we show that EDA$^+$-FN colocalizes with TLR4 on macrophages in murine aortic lesions and human coronary atherosclerotic plaques.

Materials and Methods

Materials and Methods are available in the online-only supplement.

Results

Constitutive expression of EDA$^+$-FN promotes progression of atherosclerosis, whereas deletion of EDA protects against atherosclerosis, in *Apoe*$^{-/-}$ mice

To determine the functional role of EDA$^+$-FN in atherosclerosis, we generated several novel mutant strains of *Apoe*$^{-/-}$ mice as described in methods. Both male and female *EDA*$^{-/-}$*Apoe*$^{-/-}$ mice (which lack EDA$^+$-FN), *EDA*$^{fl/fl}$*Apoe*$^{-/-}$ mice (which constitutively express EDA$^+$-FN), and control *Apoe*$^{-/-}$ mice were first fed a chow diet for 6 weeks, and then a high-fat "Western" diet for 14 weeks. Using ELISA, we first measured plasma levels of EDA$^+$-FN. As expected at baseline, EDA$^+$-FN was absent in the plasma of *EDA*$^{-/-}$*Apoe*$^{-/-}$ mice and elevated by 3-fold in *EDA*$^{fl/fl}$*Apoe*$^{-/-}$ mice compared to *Apoe*$^{-/-}$ mice ($P<0.05$, Supplementary Table I). Plasma levels of EDA$^+$-FN increased progressively after 14 weeks of high-fat "Western" diet in both *Apoe*$^{-/-}$ and *EDA*$^{fl/fl}$*Apoe*$^{-/-}$ mice but remained significantly higher in *EDA*$^{fl/fl}$*Apoe*$^{-/-}$ mice compared with *Apoe*$^{-/-}$ mice ($P<0.05$, Supplementary Table I). Irrespective of gender, plasma cholesterol and triglyceride levels were similar in the *EDA*$^{-/-}$*Apoe*$^{-/-}$, *EDA*$^{fl/fl}$*Apoe*$^{-/-}$, and *Apoe*$^{-/-}$ mice fed a high-fat diet for 14 weeks (Table 1A & 1B), suggesting that inclusion or deletion of EDA in FN does not affect plasma lipid levels. Next, we compared the extent of atherosclerosis in whole aortae by staining with Oil Red O and quantifying *en face* lesion area. Both male and female *EDA*$^{fl/fl}$*Apoe*$^{-/-}$ mice exhibited significantly larger lesion areas, whereas male and female *EDA*$^{-/-}$*Apoe*$^{-/-}$ exhibited significantly reduced lesion areas compared with male and female *Apoe*$^{-/-}$ mice ($P<0.05$, N=10-12 mice/group, Figure 1 A&1B). Next, we quantified the cross sectional area of atherosclerotic lesions in the aortic sinus using the VerHoeffs/Van Gieson staining method. We found that the mean lesion areas in the aortic sinus of both male and female *EDA*$^{fl/fl}$*Apoe*$^{-/-}$ mice were significantly larger when compared with *Apoe*$^{-/-}$ mice ($P<0.05$, Figure 1C&D). Conversely, male and female *EDA*$^{-/-}$*Apoe*$^{-/-}$ mice exhibited

significantly reduced lesion areas when compared with *Apoe* $^{-/-}$ mice (P<0.05, N=10-12 mice/group, Figure 1C&D). Next, we measured the interstitial collagen content. Picrosirius red staining of lesions in the aortic sinus revealed similar collagen content (Supplementary Figure S1) among genotypes. Additionally, plasma TNF-α and IL-1β levels were comparable among genotypes (Supplementary Figure S2).

Constitutive expression of EDA$^+$-FN increases macrophage infiltration within atherosclerotic plaques of *Apoe*$^{-/-}$ mice, whereas deletion of EDA reduces plaque inflammation

To determine whether EDA$^+$-FN enhances inflammatory cell recruitment to atherosclerotic plaques, we quantified macrophage infiltration (Mac3 positive area) within plaques of the aortic sinus by immunohistochemistry in mice fed a high-fat diet for 14 weeks. *EDA*$^{fl/fl}$*Apoe*$^{-/-}$ mice exhibited significant increase in absolute Mac3-positive area as well as % of total lesion area covered by mac3 positive cells, whereas *EDA*$^{-/-}$*Apoe*$^{-/-}$ mice had significantly reduced Mac3-positive area when compared with *Apoe*$^{-/-}$ mice (P<0.05; Figure 2A). Total leukocyte counts were similar among genotypes (Supplementary Table II).

Exogenous EDA$^+$-FN promotes uptake of native LDL complexes containing heparin and collagen

To determine whether there was a difference in uptake of modified LDL by macrophages, we incubated bone marrow-derived macrophages from *EDA*$^{fl/fl}$*Apoe*$^{-/-}$, *EDA*$^{-/-}$*Apoe*$^{-/-}$ and *Apoe*$^{-/-}$ mice with acetylated LDL (acLDL) and then stained with Oil Red O. We found that foam cell formation and acLDL uptake was comparable among *EDA*$^{fl/fl}$*Apoe*$^{-/-}$, *EDA*$^{-/-}$*Apoe*$^{-/-}$ and *Apoe*$^{-/-}$ mice after 24 hrs (Figure 2B). Additionally, foam cell formation and acLDL uptake was comparable in *EDA*$^{-/-}$*Apoe*$^{-/-}$ macrophages treated either in presence or absence of exogenous human cellular FN, which contains EDA (EDA$^+$-FN; Supplementary Figure III). Previous *in vitro* studies have suggested that fibronectin interaction with other extracellular matrix proteins such as collagen and glycosaminoglycans may enhance uptake of LDL.[24, 25] Therefore, we determined whether LDL complexes (native LDL-collagen-heparin) accumulate more in the macrophages in the presence of cFN. Interestingly, we found a significant increase in foam cell formation and LDL complex uptake in *EDA*$^{-/-}$*Apoe*$^{-/-}$ macrophages treated with LDL-heparin-collagen-cFN complexes compared to LDL-heparin-collagen complexes (Figure 2C). Foam cell formation and LDL uptake was comparable in *EDA*$^{-/-}$*Apoe*$^{-/-}$ macrophages treated with LDL or LDL-cFN (Figure 2C).

EDA$^+$-FN promotes progression of atherosclerosis via TLR4

Since EDA$^+$-FN interacts with TLR4 *in vitro*,[20] we tested the hypothesis that EDA$^+$-FN promotes progression of atherosclerosis through the TLR4 signaling pathway. We used a genetic approach and generated *Apoe*$^{-/-}$, *EDA*$^{fl/fl}$*Apoe*$^{-/-}$ and *EDA*$^{-/-}$*Apoe*$^{-/-}$ mice on a TLR4-deficient background. Controls included *Apoe*$^{-/-}$, *EDA*$^{fl/fl}$*Apoe*$^{-/-}$ and *EDA*$^{-/-}$*Apoe*$^{-/-}$ littermates, respectively. Female mice were fed a high-fat "Western" diet for 14 weeks. Deletion of TLR4 in *Apoe*$^{-/-}$, *EDA*$^{fl/fl}$*Apoe*$^{-/-}$ and *EDA*$^{-/-/}$*Apoe*$^{-/-}$ mice did not alter plasma cholesterol or triglyceride levels when compared to controls (Table 1A & 1B).

Deletion of TLR4 in *EDA*$^{fl/fl}$*Apoe*$^{-/-}$ mice significantly reduced total lesion area the aorta, as well as cross-sectional lesion area in the aortic sinus, compared with *EDA*$^{fl/fl}$*Apoe*$^{-/-}$ mice ($P<0.05$; Figure 3 A&B). Interestingly, no significant differences in plaque area in the aorta or aortic sinus were observed between *EDA*$^{-/-}$*TLR4*$^{-/-}$*Apoe*$^{-/-}$ mice and control *EDA*$^{-/-}$*Apoe*$^{-/-}$ mice (Figure 3 A&B). Together these results suggest that EDA^{+}-FN requires TLR4 for atherosclerosis exacerbation. Next, using serial sections, we measured macrophage (Mac-3 positive cells) infiltration within plaques of the aortic sinus by immunohistochemistry. Significant decrease in absolute Mac3 positive area as well % of total lesion area covered by Mac3 positive cells were observed in *EDA*$^{fl/fl}$*TLR4*$^{-/-}$*Apoe*$^{-/-}$ mice compared with control *EDA*$^{fl/fl}$*Apoe*$^{-/-}$mice ($P<0.05$, Figure 3C). Mac3 positive area was significantly decreased in *TLR4*$^{-/-}$*Apoe*$^{-/-}$ mice compared with *Apoe*$^{-/-}$ mice ($P<0.05$, Figure 3C). No significant differences in Mac3 positive area were observed between *EDA*$^{-/-}$*TLR4*$^{-/-}$*Apoe*$^{-/-}$ and EDA$^{-/-}$*Apoe*$^{-/-}$ mice (Figure 3C).

EDA^{+}-FN promotes NFkB p65 mediated inflammation in bone marrow-derived macrophages

We next determined whether the interactions of exogenous EDA^{+}-FN and TLR4 upregulate canonical NFκB p65 signaling. Bone marrow-derived macrophages from *EDA*$^{-/-}$*Apoe*$^{-/-}$ and *EDA*$^{-/-}$*TLR4*$^{-/-}$*Apoe*$^{-/-}$ mice were stimulated for 24 hrs in the presence of human cellular FN (cFN; 0-50 μg/mL), which contains the EDA. We then measured levels of phospho-NFκB p65 and NFκB p65 in cell lysates and the inflammatory cytokines TNFα and IL1β in medium. At doses of 5, 10 and 50 μg/mL of cFN, immunoblotting experiments revealed a significant linear increase in phospho-NFκB p65/total NFκB p65 levels in cFN treated macrophages from *EDA*$^{-/-}$*Apoe*$^{-/-}$ compared to control ($P<0.05$, Figure 4 A). These differences were not observed in macrophages from *EDA*$^{-/-}$*TLR4*$^{-/-}$*Apoe*$^{-/-}$ mice. Concomitantly, TNFα and IL1β protein levels were significantly increased in cFN treated macrophages from *EDA*$^{-/-}$*Apoe*$^{-/-}$, but not from *EDA*$^{-/-}$*TLR4*$^{-/-}$*Apoe*$^{-/-}$ mice, when compared with controls (Figure 4 B&C). To exclude the possibility that the *in vitro* effects were simply mediated by loss of TLR4, bone marrow-derived macrophages from *EDA*$^{-/-}$*Apoe*$^{-/-}$ and *EDA*$^{-/-}$*TLR4*$^{-/-}$*Apoe*$^{-/-}$ mice were activated with a sub-threshold dose (20 ng/mL) of phorbol myristate acetate (PMA) for 24 hrs in the presence or absence of exogenous EDA^{+}-FN (10 μg/mL). Again, we found a significant increase in phospho-NFκB p65/total NFκB p65, TNFα and IL1β protein levels in cFN treated bone marrow-derived macrophages from *EDA*$^{-/-}$*Apoe*$^{-/-}$ mice compared with untreated control *EDA*$^{-/-}$*Apoe*$^{-/-}$ mice (Figure S4). Phospho-NFκB p65/total NFκB p65, TNFα and IL1β protein levels were comparable in PMA-treated *EDA*$^{-/-}$*TLR4*$^{-/-}$*Apoe*$^{-/-}$ and *EDA*$^{-/-}$*Apoe*$^{-/-}$ macrophages, which strongly suggests that the observed *in vitro* effects were not simply mediated by TLR4 deletion, but rather by a specific effect of EDA^{+}-FN (Supplementary Figure S4).

EDA^{+}-FN colocalizes with TLR4 on macrophages in human and mice atherosclerotic plaques

To determine whether EDA^{+}-FN colocalizes with TLR4 on macrophages within human atherosclerotic plaques, we performed triple-labeling fluorescent immunostaining of autopsy samples from patients with coronary artery disease. In agreement with previous reports,[6, 18] EDA^{+}-FN was abundantly expressed within human coronary artery atherosclerotic lesions

(Figure 5A-F). Immunostaining revealed marked infiltration of Mac3- and TLR4-positive cells within the lesions, whereas staining was virtually absent in controls (P<0.0001, N=4/group, Pearson's correlation, Figure 5). Double-labeling immunostaining showed that EDA$^+$-FN colocalizes with both TLR4 (Figure 5D) and macrophages (Figure 5F). Triple-labeling immunofluorescence staining for EDA$^+$-FN, macrophages, and TLR4 suggested that EDA$^+$-FN colocalizes with TLR4 expressed on macrophages (Figure 5 A-C). Similarly, we found colocalization of EDA$^+$-FN with TLR4 on macrophages within aortic lesions of *Apoe*$^{-/-}$ mice fed a high-fat "Western' diet for 14 weeks (Figure 6).

Discussion

Although hypercholesterolemia remains a major risk factor for progression of atherosclerosis and a major therapeutic target, chronic inflammation is a critical contributor to the development of atherosclerosis. Moreover, it is widely accepted that both adaptive and innate immune receptors such as TLR4 are known to mediate progression of atherosclerosis by promoting inflammation.[23, 26, 27] We, herein, provide evidence for the first time that EDA$^+$-FN, a variant of FN that contains the alternatively-spliced EDA domain, colocalizes with TLR4 and macrophages within human coronary artery plaques and aortic lesions in atheroprone *Apoe*$^{-/-}$ mice. Furthermore, using several novel mutant strains of *Apoe*$^{-/-}$ mice, we showed that EDA$^+$-FN promotes atherosclerosis exacerbation partially through TLR4.

Despite previous evidence suggesting that EDA$^+$-FN is proatherogenic,[18, 19] the precise mechanism by which EDA$^+$-FN promotes atherosclerosis was unclear. Tan et al., proposed that reduced atherosclerosis in *EDA*$^{-/-}$*Apoe*$^{-/-}$ mice fed a high fat Western diet for 8, 12 and 16 weeks may be due to decreased total plasma cholesterol, but the differences in cholesterol levels reported were modest.[18] In another study in which atherosclerosis was induced by a atherogenic diet containing sodium cholate, Babaev et al., reported reduced atherosclerosis in both *EDA*$^{-/-}$ mice and *EDA*$^{fl/fl}$ mice compared to wild-type (C57BL/6J) mice. However, no significant differences in total cholesterol or triglyceride levels were observed between *EDA*$^{-/-}$ mice and *EDA*$^{fl/fl}$ mice fed the atherogenic diet for 8, 14, or 18 weeks.[19] Since genetically-induced atherosclerosis mouse models such as the *Apoe*$^{-/-}$ mouse are considered to be more clinically-relevant and reproducible, we generated *EDA*$^{-/-}$ mice and *EDA*$^{fl/fl}$ mice on *Apoe*$^{-/-}$ genetic background. Irrespective of gender, we found significantly reduced atherosclerosis in the aorta and aortic sinus of *EDA*$^{-/-}$*Apoe*$^{-/-}$ mice (which lack EDA$^+$-FN) and exacerbated atherosclerosis in *EDA*$^{fl/fl}$*Apoe*$^{-/-}$ mice (which constitutively express EDA$^+$-FN) when compared with control *Apoe*$^{-/-}$ mice. However, plasma cholesterol and triglyceride levels were similar among *EDA*$^{-/-}$*Apoe*$^{-/-}$, *EDA*$^{fl/fl}$*Apoe*$^{-/-}$ and *Apoe*$^{-/-}$ mice. Together these results suggest that atherosclerosis exacerbation in *EDA*$^{fl/fl}$*Apoe*$^{-/-}$ mice was not due to altered plasma cholesterol and triglyceride levels but rather due to an alternative mechanism. Indeed**,** several murine studies have shown that increased atherosclerotic lesions do not always correlate with plasma cholesterol and LDL levels**.**[28-30]

Chronic inflammation triggered by the innate immune system is recognized as a key driving force for progression of atherosclerosis.[31] Our studies show that EDA$^+$-FN promotes macrophage infiltration within atherosclerotic plaques of the aortic sinus. Intracellular and extracellular compartments contribute to lipid deposition within atherosclerotic lesions. In

animal models and in humans it is known that, within atherosclerotic lesions, monocyte-derived macrophages can take up modified extracellular lipids, thereby resulting in increased lipid deposition in the vessel wall.[27] In our studies with bone marrow-derived macrophages, we found that uptake of modified lipoproteins were comparable in *EDA*$^{fl/fl}$*Apoe*$^{-/-}$, *EDA*$^{-/-}$*Apoe*$^{-/-}$ and *Apoe*$^{-/-}$ mice. However, the *in vivo* microenvironment within the lesions in which macrophages reside is completely different compared to isolated cells. We hypothesize that the presence of EDA^{+}-FN in the arterial wall in combination with collagen and glycosaminoglycans may enhance uptake of LDL by macrophages within the lesions. Indeed, we found that exogenous cFN enhanced macrophage uptake of LDL-heparin-collagen complexes. Our findings are in agreement with previous observations that LDL when incubated with heparin, fibronectin and collagen is avidly taken by macrophages.[24, 25] Because the protein components that were used to make LDL-complexes are present in the vascular wall, we suggest that EDA^{+}-FN may potentiate foam cell formation during atherogenesis. We speculate that this could be one of the mechanisms by which *EDA*$^{fl/fl}$*Apoe*$^{-/-}$ mice are pro-atherogenic independent of alterations in plasma cholesterol or lipid levels.

Herein, we also showed for the first time the role of TLR4 in EDA^{+}-FN mediated atherosclerosis exacerbation. Previously it was demonstrated that the EDA, but not other domains, of FN activates human TLR4 expressed in HEK293 cells, which normally lack TLR4.[20] Like lipopolysaccharide, EDA activation of TLR4 requires MD-2, an accessory protein associated with extracellular domain A of TLR4 and required for TLR4-dependent LPS response.[20] We now provide *in vivo* evidence that EDA^{+}-FN promotes progression of atherosclerosis through a mechanism that is partially dependent on TLR4. Multiple endogenous ligands (e.g., heat-shock proteins, fibrinogen, and fibrin) have been shown to activate TLR4 and generate an inflammatory response. We found that TLR4 deficiency in *EDA*$^{fl/fl}$*Apoe*$^{-/-}$ or *Apoe*$^{-/-}$ mice significantly reduced lesion progression, concomitant with decreased infiltration of macrophages within the aortic sinus, although plasma cholesterol and triglyceride levels were comparable. Our results are consistent with findings from other groups who have shown that the atheroprotective effects of MyD88 or TLR4 deficiency are not due to altered serum cholesterol or lipoproteins but rather to reduced inflammation.[23] Of note, TLR4 deficiency did not significantly alter lesion size in *EDA*$^{-/-}$*Apoe*$^{-/-}$mice, suggest that EDA^{+}-FN could be one of the major endogenous ligands that promotes atherogenesis through the TLR4 signaling pathway. TLR4 is expressed on multiple cell types that might contribute to the proatherogenic role of EDA^{+}-FN. Herein, using bone marrow-derived macrophages, we demonstrate that exogenous cFN potentiated the phosphorylation of NFκB p65, which is a component of the canonical signaling pathway downstream of TLR4 and has been reported to promote atherosclerosis.[32]

Our *in vitro* studies support a mechanistic model in which lesion macrophages, through TLR4, interacts with EDA^{+}-FN in the ECM, and thereby, promote inflammatory response that may then amplify the inflammatory micro environment within atherosclerotic lesions by promoting additional monocyte entry. Although our *in vitro* mechanistic studies suggest a role for TLR4 on macrophages that may contribute to EDA^{+}-FN-mediated inflammation, and thereby, atherosclerosis exacerbation, additional murine studies employing either

endothelial- or bone marrow-specific deletion of TLR4 will be required to define the specific cell types responsible the TLR4-dependent effects of EDA^+-FN on atherosclerosis *in vivo*. Finally, we provide evidence for the first time that EDA^+-FN colocalizes with TLR4 on macrophages within human coronary atherosclerotic plaques and in murine aortic lesions. Although our studies indicate that TLR4 signaling significantly contributes to EDA^+-FN mediated inflammation during atherosclerosis, it remains possible that some of the pro-inflammatory effects of EDA^+-FN are TLR4-independent, perhaps mediated by binding sites for leukocyte integrins $\alpha4\beta1$ and $\alpha9\beta1$ in the EDA domain.[33] Additional studies will be required to determine if disruption of EDA^+-FN-integrin interactions *in vivo* prevents monocyte recruitment and subsequent atherosclerotic lesion progression.

In summary, our studies unequivocally demonstrate that EDA^+-FN is proatherogenic in mouse models of atherosclerosis. Importantly, we provide genetic evidence for the first time that EDA^+-FN/TLR4 signaling enhances recruitment of monocytes/macrophages into developing plaques, thereby promoting progression of atherosclerosis. The abundant expression of EDA^+-FN in human atherosclerotic plaques and the mechanistic insights provided by the current study may open new arenas for the prevention and treatment of atherosclerosis in patients at high risk for coronary heart disease.

Supplementary Material

Refer to Web version on PubMed Central for supplementary material.

Acknowledgments

Sources of Funding

This work was supported by National Heart, Lung, and Blood Institute (National Institutes of Health) grants R01 HL118246 and R01 HL118742 to A.K.C., RO1 HL108932 to I.M.G., and P01 HL062984 to S.R.L, and by a grant from the American Society of Hematology to S.R.L.

Non-standard Abbreviations and Acronyms

cFN	Cellular fibronectin
EDA	Extra domain A
EDA^+-FN	Cellular fibronectin containing extra domain A
TLR4	Toll-like receptor 4
ECM	Extracellular matrix
Apoe	Apolipoprotein E
acLDL	acetylated Low Density Lipoprotein

References

1. Raines EW. The extracellular matrix can regulate vascular cell migration, proliferation, and survival: Relationships to vascular disease. International journal of experimental pathology. 2000; 81:173–182. [PubMed: 10971738]

2. Strom A, Ahlqvist E, Franzen A, Heinegard D, Hultgardh-Nilsson A. Extracellular matrix components in atherosclerotic arteries of apo e/ldl receptor deficient mice: An immunohistochemical study. Histol Histopathol. 2004; 19:337–347. [PubMed: 15024695]

3. Sorokin L. The impact of the extracellular matrix on inflammation. Nat Rev Immunol. 2010; 10:712–723. [PubMed: 20865019]

4. Stenman S, von Smitten K, Vaheri A. Fibronectin and atherosclerosis. Acta Med Scand Suppl. 1980; 642:165–170. [PubMed: 6935942]

5. Shekhonin BV, Domogatsky SP, Idelson GL, Koteliansky VE, Rukosuev VS. Relative distribution of fibronectin and type i, iii, iv, v collagens in normal and atherosclerotic intima of human arteries. Atherosclerosis. 1987; 67:9–16. [PubMed: 3314885]

6. Pedretti M, Rancic Z, Soltermann A, Herzog BA, Schliemann C, Lachat M, Neri D, Kaufmann PA. Comparative immunohistochemical staining of atherosclerotic plaques using f16, f8 and l19: Three clinical-grade fully human antibodies. Atherosclerosis. 2010; 208:382–389. [PubMed: 19699478]

7. Orr AW, Sanders JM, Bevard M, Coleman E, Sarembock IJ, Schwartz MA. The subendothelial extracellular matrix modulates nf-kappab activation by flow: A potential role in atherosclerosis. The Journal of cell biology. 2005; 169:191–202. [PubMed: 15809308]

8. White ES, Baralle FE, Muro AF. New insights into form and function of fibronectin splice variants. J Pathol. 2008; 216:1–14. [PubMed: 18680111]

9. ffrench-Constant C. Alternative splicing of fibronectin--many different proteins but few different functions. Exp Cell Res. 1995; 221:261–271. [PubMed: 7493623]

10. Ffrench-Constant C, Van de Water L, Dvorak HF, Hynes RO. Reappearance of an embryonic pattern of fibronectin splicing during wound healing in the adult rat. The Journal of cell biology. 1989; 109:903–914. [PubMed: 2760116]

11. Muro AF, Chauhan AK, Gajovic S, Iaconcig A, Porro F, Stanta G, Baralle FE. Regulated splicing of the fibronectin eda exon is essential for proper skin wound healing and normal lifespan. The Journal of cell biology. 2003; 162:149–160. [PubMed: 12847088]

12. Glukhova MA, Frid MG, Shekhonin BV, Vasilevskaya TD, Grunwald J, Saginati M, Koteliansky VE. Expression of extra domain a fibronectin sequence in vascular smooth muscle cells is phenotype dependent. The Journal of cell biology. 1989; 109:357–366. [PubMed: 2663879]

13. Takasaki I, Chobanian AV, Mamuya WS, Brecher P. Hypertension induces alternatively spliced forms of fibronectin in rat aorta. Hypertension. 1992; 20:20–25. [PubMed: 1618548]

14. Coito AJ, Brown LF, Peters JH, Kupiec-Weglinski JW, van de Water L. Expression of fibronectin splicing variants in organ transplantation: A differential pattern between rat cardiac allografts and isografts. Am J Pathol. 1997; 150:1757–1772. [PubMed: 9137099]

15. Muro AF, Moretti FA, Moore BB, Yan M, Atrasz RG, Wilke CA, Flaherty KR, Martinez FJ, Tsui JL, Sheppard D, Baralle FE, Toews GB, White ES. An essential role for fibronectin extra type iii domain a in pulmonary fibrosis. Am J Respir Crit Care Med. 2008; 177:638–645. [PubMed: 18096707]

16. Jarnagin WR, Rockey DC, Koteliansky VE, Wang SS, Bissell DM. Expression of variant fibronectins in wound healing: Cellular source and biological activity of the eiiia segment in rat hepatic fibrogenesis. The Journal of cell biology. 1994; 127:2037–2048. [PubMed: 7806580]

17. Barnes JL, Hastings RR, De la Garza MA. Sequential expression of cellular fibronectin by platelets, macrophages, and mesangial cells in proliferative glomerulonephritis. Am J Pathol. 1994; 145:585–597. [PubMed: 8080041]

18. Tan MH, Sun Z, Opitz SL, Schmidt TE, Peters JH, George EL. Deletion of the alternatively spliced fibronectin eiiia domain in mice reduces atherosclerosis. Blood. 2004; 104:11–18. [PubMed: 14976060]

19. Babaev VR, Porro F, Linton MF, Fazio S, Baralle FE, Muro AF. Absence of regulated splicing of fibronectin eda exon reduces atherosclerosis in mice. Atherosclerosis. 2008; 197:534–540. [PubMed: 17897651]

20. Okamura Y, Watari M, Jerud ES, Young DW, Ishizaka ST, Rose J, Chow JC, Strauss JF 3rd. The extra domain a of fibronectin activates toll-like receptor 4. J Biol Chem. 2001; 276:10229–10233. [PubMed: 11150311]

21. Khan MM, Gandhi C, Chauhan N, Stevens JW, Motto DG, Lentz SR, Chauhan AK. Alternatively-spliced extra domain a of fibronectin promotes acute inflammation and brain injury after cerebral ischemia in mice. Stroke. 2012; 43:1376–1382. [PubMed: 22363055]
22. Bhattacharyya S, Tamaki Z, Wang W, Hinchcliff M, Hoover P, Getsios S, White ES, Varga J. Fibronectineda promotes chronic cutaneous fibrosis through toll-like receptor signaling. Sci Transl Med. 2014; 6:232ra250.
23. Michelsen KS, Wong MH, Shah PK, Zhang W, Yano J, Doherty TM, Akira S, Rajavashisth TB, Arditi M. Lack of toll-like receptor 4 or myeloid differentiation factor 88 reduces atherosclerosis and alters plaque phenotype in mice deficient in apolipoprotein e. Proc Natl Acad Sci U S A. 2004; 101:10679–10684. [PubMed: 15249654]
24. Falcone DJ, Mated N, Shio H, Minick CR, Fowler SD. Lipoprotein-heparin-fibronectin-denatured collagen complexes enhance cholesteryl ester accumulation in macrophages. The Journal of cell biology. 1984; 99:1266–1274. [PubMed: 6480690]
25. Falcone DJ, Salisbury BG. Fibronectin stimulates macrophage uptake of low density lipoprotein-heparin-collagen complexes. Arteriosclerosis. 1988; 8:263–273. [PubMed: 3370022]
26. Michelsen KS, Doherty TM, Shah PK, Arditi M. Role of toll-like receptors in atherosclerosis. Circ Res. 2004; 95:e96–97. [PubMed: 15591233]
27. Rosenfeld ME. Inflammation and atherosclerosis: Direct versus indirect mechanisms. Current opinion in pharmacology. 2013; 13:154–160. [PubMed: 23357128]
28. Boring L, Gosling J, Cleary M, Charo IF. Decreased lesion formation in ccr2−/− mice reveals a role for chemokines in the initiation of atherosclerosis. Nature. 1998; 394:894–897. [PubMed: 9732872]
29. Wang Y, Wang GZ, Rabinovitch PS, Tabas I. Macrophage mitochondrial oxidative stress promotes atherosclerosis and nuclear factor-kappab-mediated inflammation in macrophages. Circ Res. 2014; 114:421–433. [PubMed: 24297735]
30. Gandhi C, Khan MM, Lentz SR, Chauhan AK. Adamts13 reduces vascular inflammation and the development of early atherosclerosis in mice. Blood. 2012; 119:2385–2391. [PubMed: 22123843]
31. Hansson GK, Hermansson A. The immune system in atherosclerosis. Nat Immunol. 2011; 12:204–212. [PubMed: 21321594]
32. de Winther MP, Kanters E, Kraal G, Hofker MH. Nuclear factor kappab signaling in atherogenesis. Arterioscler Thromb Vasc Biol. 2005; 25:904–914. [PubMed: 15731497]
33. Liao YF, Gotwals PJ, Koteliansky VE, Sheppard D, Van De Water L. The eiiia segment of fibronectin is a ligand for integrins alpha 9beta 1 and alpha 4beta 1 providing a novel mechanism for regulating cell adhesion by alternative splicing. J Biol Chem. 2002; 277:14467–14474. [PubMed: 11839764]

Significance

EDA$^+$-FN isoforms are abundant in the ECM of atherosclerotic arteries but absent from healthy arteries. We show that exogenous cellular FN stimulates macrophage uptake of LDL-heparin-collagen complexes suggesting that ECM rich in EDA$^+$-FN may play a role in cellular lipid accumulation in atherosclerotic lesions. Additionally, we demonstrate for the first time that EDA$^+$-FN colocalizes with TLR4 on macrophages in human coronary artery atherosclerotic plaques suggesting a pro-inflammatory role for EDA$^+$-FN in atherosclerosis exacerbation. The abundant presence of EDA$^+$-FN in human atherosclerosis and the mechanistic insights provided by the current study raises possibility to target EDA$^+$-FN that may show benefit in patients at high risk of atherosclerosis.

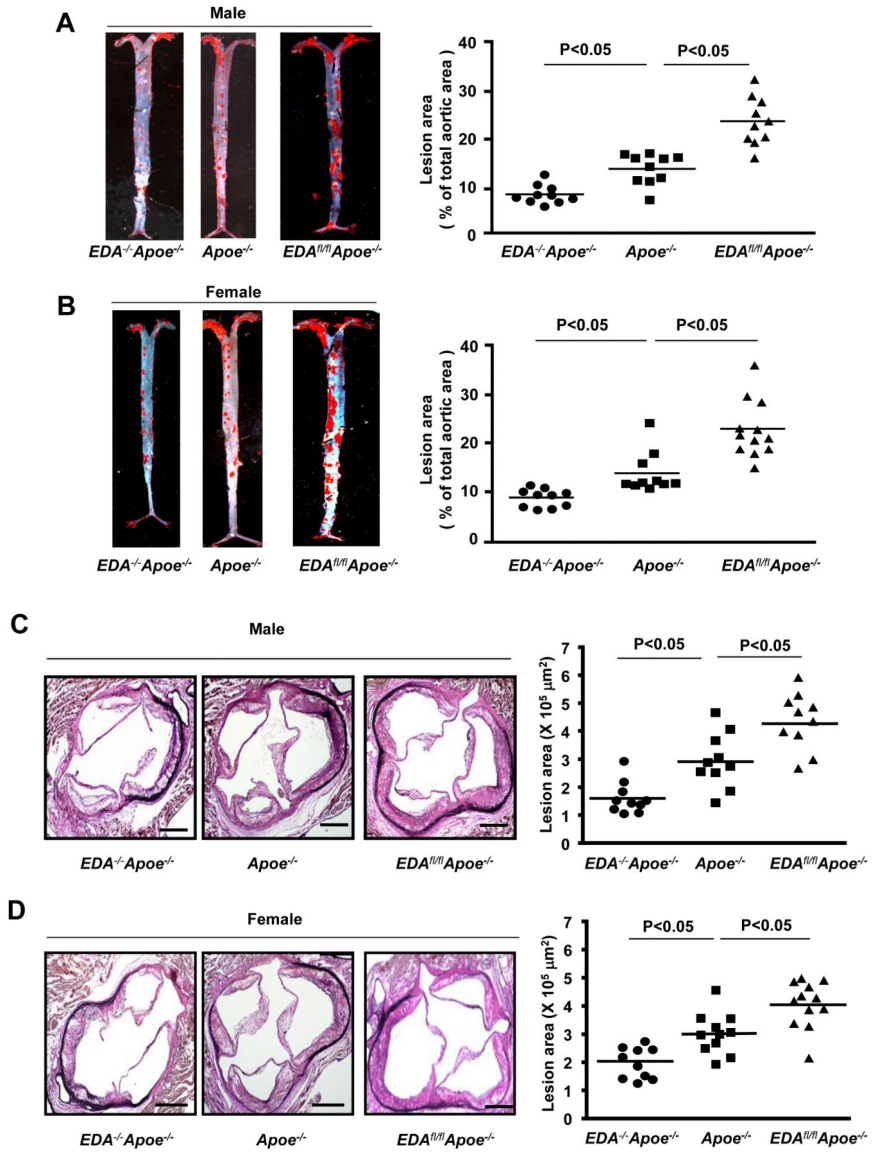

Figure 1. EDA^{+}-FN promotes early atherosclerotic lesion formation in the aorta and aortic sinus

EDA$^{-/-}$*Apoe*$^{-/-}$, *EDA*$^{fl/fl}$*Apoe*$^{-/-}$, and control *Apoe*$^{-/-}$ mice were fed a high-fat Western diet for 14 weeks. **A&B.** Left panel shows Oil red O staining of the representative aortae. Right panel shows quantification of en face lesion area **C&D.** Left panel shows representative photomicrographs of VerHoeffs/Van Geison-stained aortic sinuses. Scale bar = 200µm. Right panel shows quantification of lesion in the cross section area of aortic sinuses. Each dot represents a single mouse. Horizontal bars indicate mean values. N=10-12 mice/group.

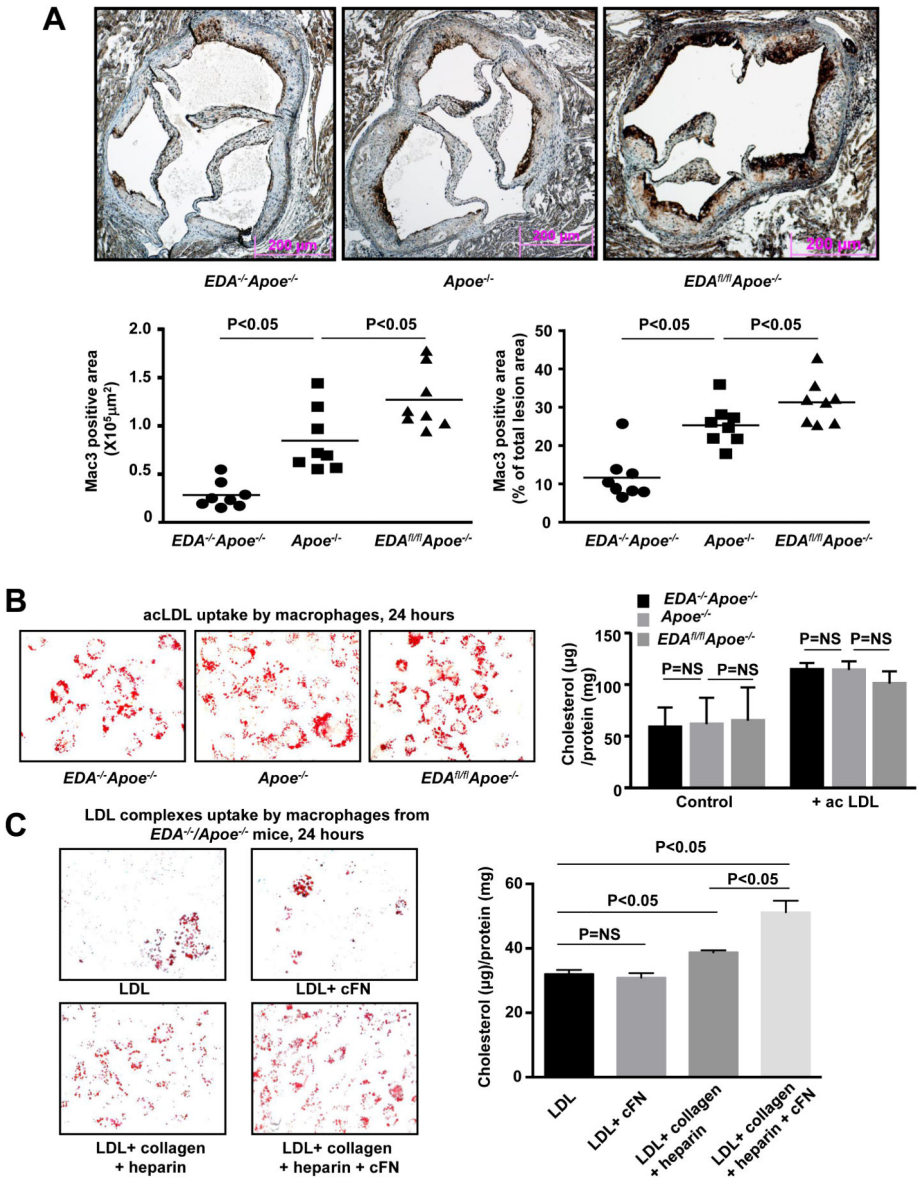

Figure 2. EDA^{+}-FN enhances macrophage cells infiltration but not foam cell formation

A. Top panel shows representative photomicrographs stained for macrophages (mac-3 positive cells stained as brown) and counterstained with hematoxylin (blue). Scale bar = 200µm. Bottom panel shows quantification. N=8 mice/group. Each dot represents a single mouse. Value for each mouse represents a mean of 16 fields from 4 serial sections (each 80 mm apart, beginning at the aortic valve leaflets and spanning 320 mm). **B.** Left panel shows staining of purified bone marrow-derived macrophages from female *EDA*$^{-/-}$*Apoe*$^{-/-}$, *EDA*$^{fl/fl}$*Apoe*$^{-/-}$, and control *Apoe*$^{-/-}$ mice with Oil Red O 24 hour after incubating them with acetylated LDL (100 µg/ml). Right panel shows quantification of total cholesterol. **C**. Left panel shows staining of purified bone marrow-derived macrophages from female *EDA*$^{-/-}$*Apoe*$^{-/-}$ mice with Oil Red O 24 hour after incubating them with LDL (50 µg/ml) under different conditions. Right panel shows quantification of total cholesterol. Values are mean ± SEM. N=5-6 mice/group. NS= non significant.

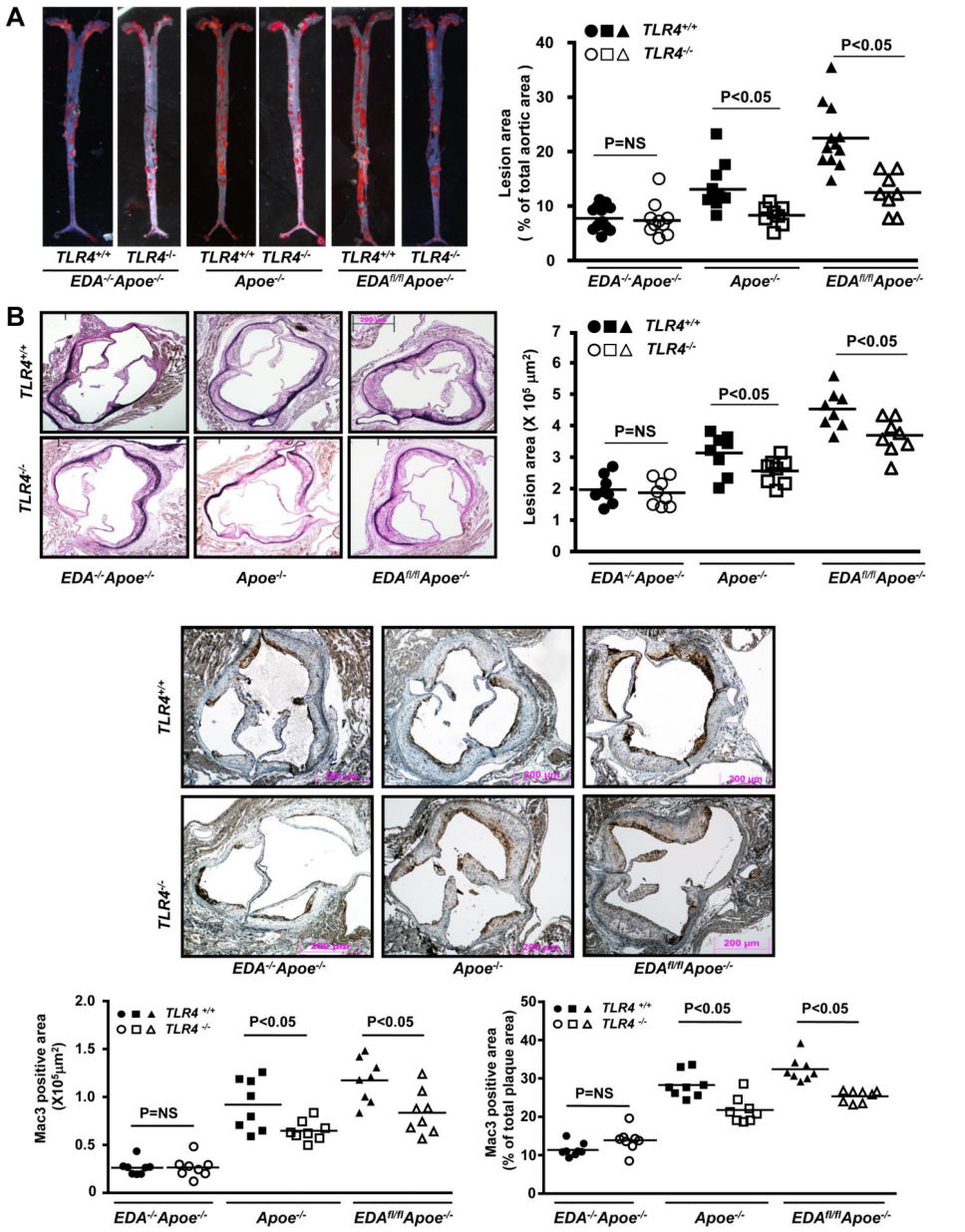

Figure 3. TLR4 contributes to EDA$^+$-FN-mediated accelerated atherosclerosis in the aorta and aortic sinus of female mice fed a high-fat "Western" diet for 14 weeks

A. Left panel shows Oil red O staining of the representative aortae. Right panel shows quantification of en face lesion (N=8-12 mice/group). **B**. Left panel shows representative photomicrographs of VerHoeffs/Van Geison-stained aortic sinuses. Scale bar = 200µm. Right panel shows quantification of lesion in the cross section area of aortic sinuses (N=8-10 mice/group). **C.** Top panel shows representative photomicrographs stained for macrophages (Mac-3 positive cells stained as brown). All the sections were counterstained with Hematoxylin (blue). Scale bar = 200µm. Bottom panel shows quantification of Mac3 positive area. N=8 mice/group. Each dot represents a single mouse.

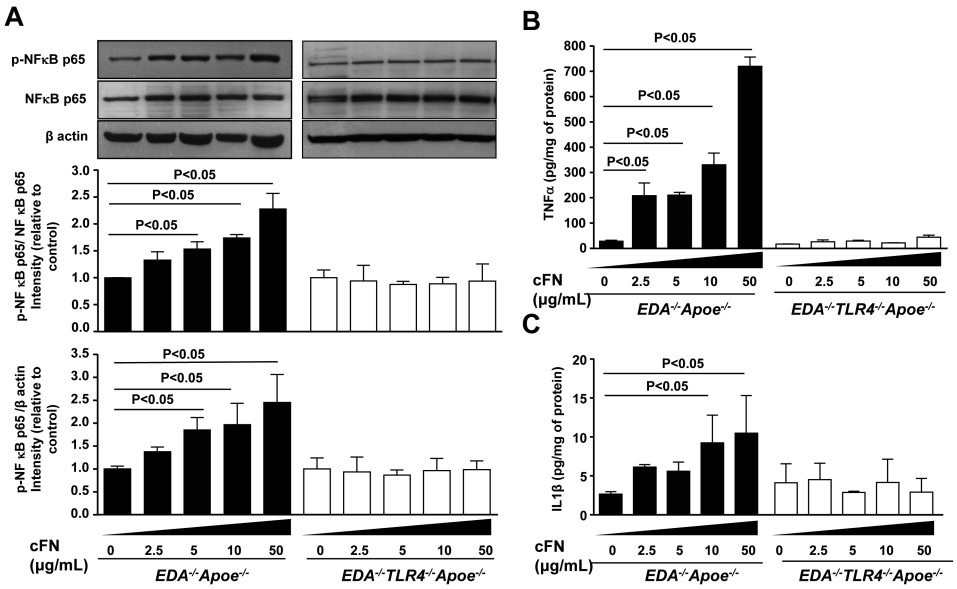

Figure 4. Dose dependent effect of exogenous cFN on TLR4-mediated inflammation in macrophages

Pooled bone marrow-derived macrophages from *EDA*$^{-/-}$*Apoe*$^{-/-}$ and *EDA*$^{-/-}$*TLR4*$^{-/-}$*Apoe*$^{-/-}$ mice (n=4-5 mice/group) were stimulated in presence of cFN (0-50 μg/mL) for 24 hours. **A.** Top panel shows representative immunoblots showing expression of phosphorylated- NFkB p65, total NFkB p65 and β-actin. Bar diagram in middle and bottom panels represent quantification of intensity of phosphorylated- NFkB p65 to total NFkB p65 and phosphorylated- NFkB p65 to β-actin (loading control). N = 3 experiments/ group. **B&C**. ELISA quantification of TNF-α and IL-1β in supernatant medium from cFN treated and untreated macrophages. Data is presented as mean ± SEM. N = 3 experiments/ group.

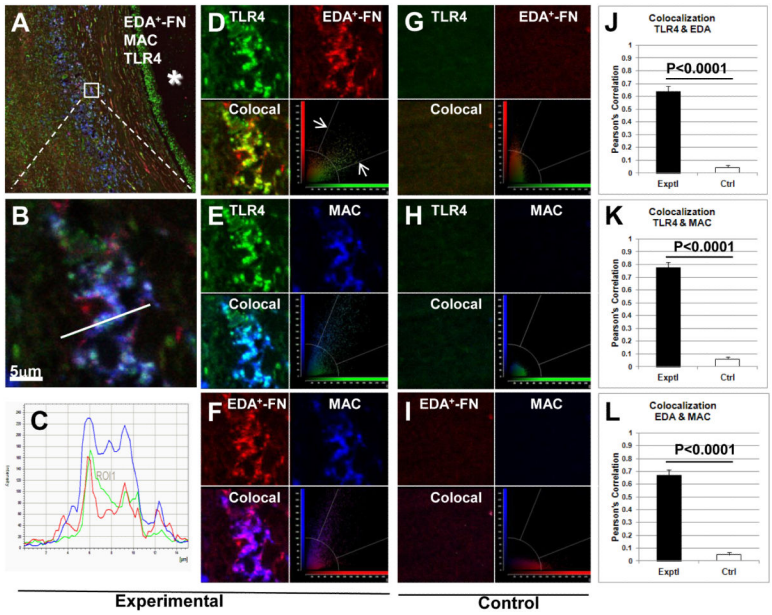

Figure 5. Colocalization of TLR4, EDA$^+$-FN, and Mac3 in human atherosclerotic plaques

Confocal images showing triple-immunostaining for TLR4 (green), EDA$^+$-FN (red), and Mac3 (blue) in atherosclerotic (A-F) and control healthy (G-I) human tissue sections. **A.** Low-magnification image showing staining in the vessel wall relative to the lumen (*). **B.** Higher magnification image showing co-localization in the boxed region shown in panel A. **C.** Plot profile shows co-localization of fluorescence signal for TLR4, EDA$^+$-FN, and Mac3 along the line shown in panel B. **D-I.** Quantitative analysis of pairs of images show co-localization for TLR- EDA$^+$-FN (D, G, J), TLR4-Mac3 (E, H, K) and EDA$^+$-FN-Mac3 (F, I, L). Co-localized pixels are defined as those whose intensity values for both channels fell within a pre-set range above the background intensity level (white arrows as shown in figure D). The field of view in a control tissue section (G-I) is at a comparable location relative to the vessel lumen. **J-L.** Co-localization (Pearson's Correlation, 1 = complete co-localization). N = 4/condition.

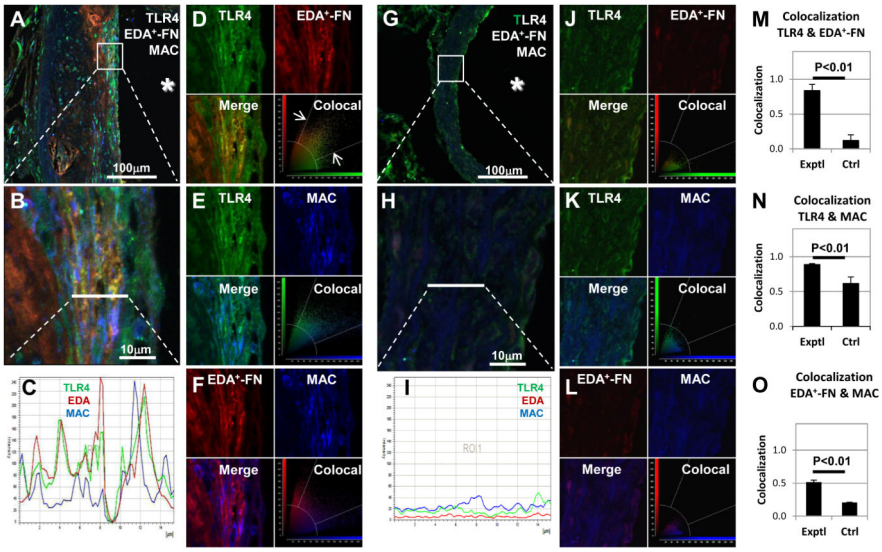

Figure 6. Colocalization of TLR4, EDA, and MAC in aortic lesions of Apoe$^{-/-}$ mice fed a high-fat "Western" diet (A-F) and chow diet (G-L) for 14 weeks

Confocal images showing triple-immunostaining for TLR4 (green), EDA (red), and MAC (blue). **A,G**. Low-mag images showing staining in the vessel wall relative to the lumen (*).**B,H.** Higher magnification images showing colocalization in the boxed region shown in panel A/G. **C, I.** Plot profile shows colocalization of fluorescence signal for TLR4 (green), EDA (red), and MAC (blue) along the line shown in panel B/H. **M-O**. Quantitative analysis of pairs of images show colocalization for TLR-EDA (D,J), TLR4-MAC (E,K), and EDA-MAC (F,L). Colocalized pixels are defined as those whose intensity values for both channels fell within a pre-set range above the background intensity level (white arrows in D). Colocalization rate (1 = complete colocalization). N = 3/group.

Table 1A

Plasma total cholesterol and triglyceride levels in male mice fed a high-fat “Western” diet for 14 weeks.

Strains	Total cholesterol levels (mg/dL)	P value versus *Apoe*$^{-/-}$	Triglycerides levels (mg/dL)	P value versus *Apoe*$^{-/-}$
Apoe $^{-/-}$	597 ± 54		186 ± 11	
EDA $^{-/-}$ *Apoe* $^{-/-}$	645 ± 57	P=0.8	211 ± 32	P=0.7
EDA$^{fl/fl}$ *Apoe* $^{-/-}$	585 ± 58	P=0.7	201 ± 16	P=0.2
TLR4 $^{-/-}$ *Apoe* $^{-/-}$	535 ± 53	P=0.6	183 ± 16	P=0.8
EDA $^{-/-}$ *TLR4* $^{-/-}$ *Apoe* $^{-/-}$	593 ± 85	P=0.4	196 ± 19	P=0.7
EDA$^{fl/fl}$ *TLR4* $^{-/-}$ *Apoe* $^{-/-}$	604 ± 60	P=0.8	177 ± 24	P=0.6

Values are represented as means ± SEM. N=8-10/group.

Table 1B

Plasma total cholesterol and triglyceride levels in female mice fed a high-fat “Western” diet for 14 weeks.

Strains	Total cholesterol levels (mg/dL)	P value versus *Apoe*$^{-/-}$	Triglycerides levels (mg/dL)	P value versus *Apoe*$^{-/-}$
Apoe $^{-/-}$	492 ± 57		123 ± 8	
EDA $^{-/-}$ *Apoe* $^{-/-}$	433 ± 52	P=0.5	101 ± 11	P=0.1
EDA$^{fl/fl}$ *Apoe* $^{-/-}$	429 ± 35	P=0.4	107 ± 6	P=0.2
TLR4 $^{-/-}$ *Apoe* $^{-/-}$	450± 36	P=0.6	110 ±16	P=0.3
EDA $^{-/-}$ *TLR4* $^{-/-}$ *Apoe* $^{-/-}$	488 ± 46	P=0.9	125 ± 14	P=0.3
EDA$^{fl/fl}$ *TLR4* $^{-/-}$ *Apoe* $^{-/-}$	402 ± 51	P=0.2	117 ± 22	P=0.3

Values are represented as means ± SEM. N=8-10/group.